Electronic Supplementary Information

for

Combinatorial approaches for developing upconverting nanomaterials: High-throughput screening, modeling, and applications

Emory M. Chan*

The Molecular Foundry, Lawrence Berkeley National Laboratory, Berkeley, CA 94720, USA

* To whom correspondence should be addressed. E-mail: EMChan@lbl.gov

---

Table of Contents

S1 Calculating rate constants for lanthanide transitions

1.1 Judd-Ofelt theory

Judd-Ofelt (JO) theory[1,2] is used to calculate the radiative rates of $4f^N$ manifold-to-manifold electric dipole (ED) transitions in lanthanide ions.[3,4] According to the theory,[1-4] the rate constant (in s^{-1}) for electric dipole radiative relaxation, A_{ij}^{ED}, can be determined using the three JO parameters (Ω_λ) and the doubly reduced matrix elements of the unit tensor operator $U^{(\lambda)}$ of rank λ, where λ=2,4, or 6:

$$A_{ij}^{ED} = \frac{64\pi^4 e^2 \tilde{\nu}^3}{3h(2J+1)} \left[\frac{n\left(n^2+2\right)^2}{9} \right] S_{ij}^{ED} \qquad (S1)$$

$$S_{ij}^{ED} = \sum_{\lambda=2,4,6} \Omega_\lambda \left| \left\langle [SL]J_i \left\| U^{(\lambda)} \right\| [SL]J_j \right\rangle \right|^2 \qquad (S2)$$

Here, $\tilde{\nu}$ is the energy of the transition in wavenumbers, h is Planck's constant, e is the elementary charge, n is the index of refraction of the material, J is the total angular momentum of the initial state, and S_{ij}^{ED} is the electric dipole line strength, using the Gaussian unit system. The reduced matrix elements are typically treated as independent of the host material and are retrieved from tables in the literature, e.g. from Carnall *et al.*[3-5] or Kaminskii.[6] The empirical Ω_λ parameters are dependent on the material and can be fit from absorption or emission spectra.

For absorption, $A_{ij} = \phi\sigma_{ij}$, where ϕ is the incident photon flux. The ED absorption cross section of the transition, σ_{ij}^{ED}, can be derived from S_{ij}^{ED} using the relation:[4]

$$\sigma_{\text{int}}^{ED} = \int_{manifold} \sigma_{ij}^{ED}(\nu)\, d\nu = \frac{8\pi^3 e^2 \tilde{\nu}}{3hcg_i} \frac{\left(n^2+2\right)^2}{9n} S_{ij}^{ED} \qquad (S3)$$

Here, σ_{int}^{ED} is the ED absorption cross section integrated over the entire transition. Since coherent excitation sources typically have narrower line widths than UCNP absorption peaks, σ_{ij}^{ED} is determined from σ_{int}^{ED} using observed or assumed line shapes.

1.2 Magnetic dipole radiative transitions

Magnetic dipole (MD) radiative rate constants A_{ij}^{MD} can be calculated with the equations:

$$A_{ij}^{MD} = \frac{64\pi^4 e^2 \tilde{\nu}^3}{3h(2J+1)} n^3 S_{ij}^{MD} \qquad (S4)$$

$$S_{ij}^{MD} = \mu_B{}^2 \left| \left\langle [SL]J_i \middle\| \mathbf{L} + 2\mathbf{S} \middle\| [SL]J_j \right\rangle \right|^2 \qquad (S5)$$

where μ_B is the Bohr magneton. **L** and **S** are the angular momentum and spin operators, respectively. The matrix elements of **L** + 2**S** are tabulated by Weber[7] and others. The prominent magnetic dipole transitions of lanthanide ions and their transition rates are tabulated by Dodson and Zia.[8] The integrated MD absorption cross section and oscillator strength are calculated using the expressions below:

$$\sigma_{\text{int}}^{MD} = \frac{\pi e^2}{mc^2} f_{ij}^{MD} \qquad (S6)$$

$$f_{ij}^{MD} = \frac{8\pi^2 mc\tilde{\nu}}{3he^2 g_i} n S_{ij}^{MD} \qquad (S7)$$

Here, σ_{int}^{MD} is the MD absorption cross section integrated over the entire transition. f_{int}^{MD} is the corresponding the MD oscillator strength.

1.3 Phonon-assisted energy transfer

Kushida[9] derived an expression for the orientation-averaged rate of dipole-dipole energy transfer between a donor and acceptor. Here, the rate $W_{ij,kl}^{ET}$ of ET with donor transition $i \rightarrow j$ and acceptor transition $k \rightarrow l$ is described as a function of the inter-ion distance R and the ED line strengths S^{ED} of the donor and acceptor transitions:[1,2]

$$W_{ij,kl}^{ET} = \frac{C_{DA,ijkl}}{R^6} \qquad (S8)$$

$$C_{DA,ijkl} = \frac{8\pi^2 e^4 s_0}{3h^2 c g_i g_k} \left(\frac{n^2+2}{3n} \right)^4 S_{ij}^{ED} S_{kl}^{ED} \qquad (S9)$$

In this expression, C_{DA} is the energy transfer micro-parameter, g_i is the $2J$+1 number of states in manifold i, and s_0 is the overlap integral between the normalized donor emission spectrum and acceptor absorption spectrum.

To account for phonon assistance during non-resonant energy transfer, Miyakawa and Dexter[32] modified the expression for resonant energy transfer rates with an exponential dependence analogous to the Energy Gap Law. The phonon-assisted energy transfer micro-parameter can then be expressed as:

$$C_{DA}^{PAET} = C_{DA}^{0} \exp[-\beta_{MPR} \Delta E] \qquad (S10)$$

where β_{MPR} is a material-dependent constant related to the MPR constant α,[10] and ΔE is the net energy difference between the donor and acceptor transitions. C_{DA}^{0} is the energy transfer microparameter assuming a resonant ET process.

To account for energy transfer over all possible donor-acceptor distances R in a nanocrystal, the total phonon-assisted energy transfer (PAET) rate constant for a given donor can be calculated by integrating Eq. S8 over all R,[11] i.e.:

$$W_{ij,kl,avg}^{PAET} = N_A \int_{R_{\min}}^{\infty} \frac{C_{DA}^{PAET}}{R^6} g(R) 4\pi R^2 dR \qquad (S11)$$

where N_A is the population of the acceptor, C_{DA}^{PAET} is the PAET micro-parameter, $g(R)$ is the radial distribution function (RDF) of acceptors at a distance R from the donor, and R_{min} is the minimum donor-acceptor distance allowed by the crystal structure of the host matrix. In the case of a homogeneously doped material, $g(R)$=1, and Eq. S11 reduces to:

$$W_{ij,kl,avg}^{PAET} = \frac{4\pi}{3} N_A C_{DA}^{PAET} R_{\min}^{-3} = N_A P_{ij,kl}^{MAET} \qquad (S12)$$

To make the rate constant independent from the acceptor population, Eq. 2 in the main text uses the constant, $P_{ij,kl}^{MAET}$ (units of cm^3), whose relationship with $W_{ij,kl,avg}^{MAET}$ is shown above.

An isotropic distribution of acceptors typically is only found in liquid solutions and not in crystalline hosts. The RDF and $P_{ij,kl}^{MAET}$ for various crystals can be calculated numerically. The assumption of an isotropic distribution also implies that energy transfer events do not locally deplete donors and acceptors. This assumption is valid at the high dopant concentrations (~1 mol %) typical for upconverting nanoparticles. In this "fast migration" regime, resonant energy transfer between donors is significantly faster than phonon-assisted energy transfer between a donor and acceptor, such that excited donors redistribute themselves rapidly between energy transfer events.

Eq. S12 also holds in the opposite regime at low dopant concentrations that prevent migration, assuming that the dopant distribution is isotropic.[12] In the intermediate migration regime, donor-acceptor energy transfer rates are a convolution of donor-donor and donor-acceptor energy transfer microparameters.[12-14]

S2 Supplemental Figure S1

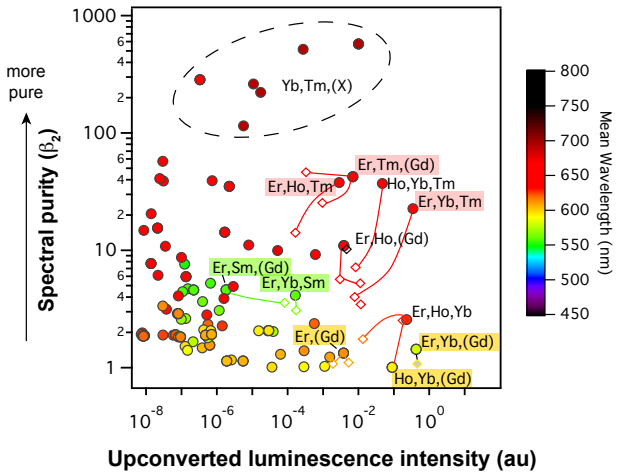

Figure S1. Combinatorial *in silico* screening of $NaYF_4$ nanocrystals doped with three lanthanide ions. Spectral purity (β_2) vs intensity for $NaYF_4$ nanocrystals calculated for UCNPs doped with 2 mol % in each ion and excited at 980 nm (10 W/cm^2). Simulated points (filled circles) are linked with a solid line to experimental values (hollow diamonds) from Figure 11.[15] Experimental intensities were normalized based on the calculated intensity of Yb^{3+}/Er^{3+}. Color scale indicates the mean weighted wavelength of each point. Dashed oval contains simulated Yb^{3+}/Tm^{3+} samples whose dominant peak is centered at 800 nm, outside of the experimental spectral range.

S3 Supplemental Figure S2

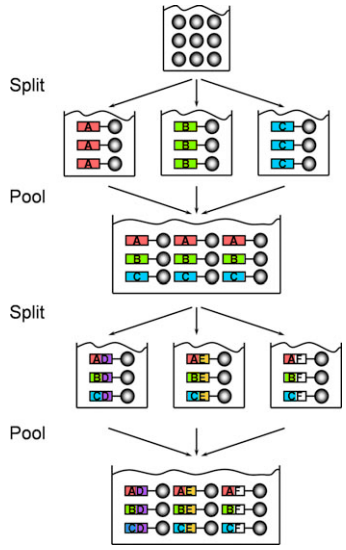

Figure S2. Generation of diverse material libraries via the Split-and-Pool method. Reprinted from Klein *et al.*,[16] Copyright 2003, with permission from Elsevier.

S4 Supplemental references

1. B. R. Judd, *Phys. Rev.*, 1962, **127**, 750–761.
2. G. S. Ofelt, *J. Chem. Phys.*, 1962, **37**, 511–520.
3. M. P. Hehlen, M. G. Brik, and K. W. Krämer, *J. Lumin.*, 2013, **136**, 221–239.
4. B. M. Walsh, in *Advances in Spectroscopy for Lasers and Sensing*, eds. B. Di Bartolo and O. Forte, Springer, Netherlands, 2006, pp. 400–433.
5. W. T. Carnall, H. Crosswhite, and H. M. Crosswhite, *Energy Level Structure and Transition Probabilities in the Spectra of the Trivalent Lanthanides in LaF3*, DOE Report #ANL-78-XX-95, Argonne National Laboratory, 1977.
6. A. A. Kaminskii, *Crystalline Lasers*, CRC Press, Boca Raton, FL, 1996.
7. B. Walsh, N. Barnes, and B. Di Bartolo, *J. Appl. Phys.*, 1998, **83**, 2772–2787.
8. C. M. Dodson and R. Zia, *Phys. Rev. B*, 2012, **86**, 125102.
9. T. Kushida, *J. Phys. Soc. Jpn.*, 1973, **34**, 1318–1326.
10. T. Miyakawa and D. Dexter, *Phys. Rev. B*, 1970, **1**, 2961–2969.
11. F. Auzel and F. Pelle, *Phys. Rev. B*, 1997, **55**, 11006–11009.
12. B. Di Bartolo, *Energy Transfer Processes in Condensed Matter*, Plenum Press, New York, 1983.
13. M. Weber, *Phys. Rev. B*, 1971, **4**, 2932–2939.
14. M. Yokota and O. Tanimoto, *J. Phys. Soc. Jpn.*, 1967, **22**, 779–784.
15. E. M. Chan, G. Han, J. D. Goldberg, D. J. Gargas, A. D. Ostrowski, P. J. Schuck, B. E. Cohen, and D. J. Milliron, *Nano Letters*, 2012, **12**, 3839–3845.
16. J. Klein, T. Zech, J. M. Newsam, and S. A. Schunk, *Applied Catalysis A: General*, 2003, **254**, 121–131.